

Design and Simulation of Parallel Manipulator for Vehicle Driving Simulator

Khalid Ali Abdelaziz Ali¹, Liu Ying²

¹Tianjin University of Technology and Education, Dagu Nanlu Road, Tianjin, China

²Professor, Tianjin University of Technology and Education, Dagu Nanlu Road, Tianjin, China

Abstract: A 3-Dof RPS parallel manipulator is selected in order to realize the motion of the driver simulator. For every limb, the structural designs are carried, which include the screw shaft and nut calculation, the load calculation, the motors selection, and so on. According to calculation, a model is established by using UG 6.0. modeling simulation in ADAMS software It supplied the basis for the further research.

Keywords: degree of freedom ; joints desgin; nut selection; motor specifications selection; desgin and modeling; simulation using ADAMS

1. Introduction

The design of parallel manipulators can be trace back to 1962, when Gough and Whitehall (1962) devised a six-linear jack system for used as a universal tire- testing machine. Stewart (1965) designs a platform manipulator for use as an aircraft simulator in 1965. Since then a systematic study of the kinematic structure of parallel manipulators in 1983 was performed by Hunt (1983). Parallel manipulators have been studied extensively by numerous researchers (Clearly and Arai, 1991; Fitcher , 1986; Grffis and Duffy, 1989; Innocenti and Parenti-Castelli, 1990; Mohamed and Duffy, 1985; Nanua et al., 1990; Zhang and Song, 1994) [1]

Parallel platform is gaining popularity and widely used in many applications with the development and application of virtual reality technology which include among others, vehicle driving simulator, parallel kinematic machine, flight simulator, simulation of seismic waves, pointing and polishing machine and earthquake wave simulator etc. Moreover, it continue to expand into new application areas[2] .Parallel manipulator is a field of interest for a many researchers due its diversified applications, high accuracy and speed more than serial manipulator.

Researchers are battling to come up with new ideas on how to deal with the working space problem of the manipulator without compromising the other design parameters. Its accuracy and repeatability is an attribute to its high stiffness and low inertia and also it has great ability to withstand heavy load due to the fact that the load is merely assumed to be distributed to the platform which in turn the platform is supported by limbs., the parallel robots consists of fixed base which might be of various shapes depend on designers choice and applications intended to performed, but usually the base shape is not playing an important role during the application. Attached to the base are limbs which is an assembly of more than one joint, the joint assembly also depend on the designers choice. Attached to the limbs of the parallel robot is the moving platform which served as end effectors[1] .

Because parallel manipulator has characteristics as above, it is able to be used as vehicle driving simulator. When it is used as vehicle driving manipulator, there are many advantages such as low cost, professional driver training, high precision, safety, and so on.

2. Degree of Freedom of Parallel Manipulator

For the vehicle driving simulator which the given parameters are listed in Table 1, a spatial 3-DOF, RPS parallel manipulator (shown in Figure 1) is selected. As shown, three identical limbs connect the moving platform by spherical joints and fixed base by revolute joints. And each limb consists of an upper member and lower member connected by a prismatic joint. Ball screws can be used to vary the lengths of the prismatic joints and therefore to control the location of the moving platform [3]

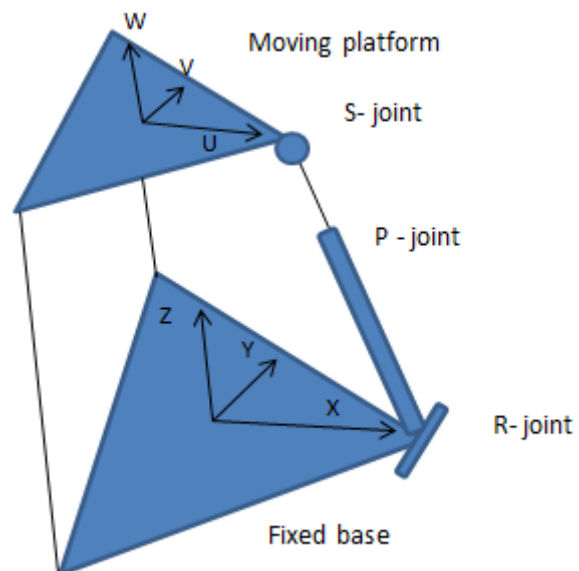


Figure 1: spatial 3-dof 3RPS parallel manipulator

$$F = \lambda(n-j-1) + \sum_{i=1}^j f_i - f_p \quad (1)$$

Where, F is degrees of freedom of a mechanism. f_i is degrees of relative motion permitted by joint i. j is number of joints in a

mechanism. n is number of links in a mechanism. λ is degrees of freedom of the space in which a mechanism is intended to function. f_p is number of passive degrees of freedom in a mechanism.

So from figure (3) using formal (1)

$$F = \lambda(n-j-1) + \sum f_i - f_p = 3DOF$$

So, it is a symmetrical manipulator, which the number of degree of freedom is equal to the number of limbs which is equal to the total number of loops of that manipulator.

Table 1: The given parameters

quantity	symbol
Mass	m
Stroke length	ls
Maximum Velocity	Vmax
Time for Speed up	t1
Time for Speed down	t3
Frequency	n
Work Life hours	h
AC Servo Motor	N
Transmission Ratio	i
Friction factor on Guide Face	μ
Resistance Force on Guide Face	f
Inertia Torque of Motor	Jm

3. Structural Design of Prismatic Joint

A screw shaft is chosen to realize the motion of prismatic joint. Its design majors in the following ways.

3.1 Lead and Shaft Diameter design

As shown in Figure 3, lead means advance of the nut along the length of the screw per revolution, Screw shaft diameter meanings largest diameter over the threaded section (at top of threads), root diameter meanings smallest diameter over the threaded section (at base of threads).

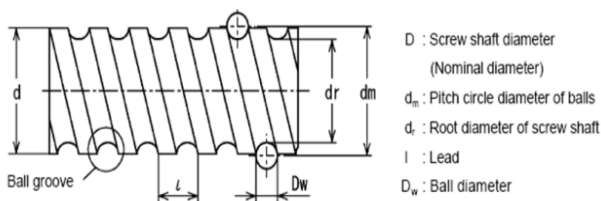


Figure 2: Screw shaft

Using equation (2) to calculate the lead:
 rotational speed (rev per min) = Linear velocity (mm per min) / Lead (mm per rev) (2)

So lead is = $V_{max}/N = 18\text{mm}$

From the table (2) below, 20mm lead is chosen which correspond to the 36mm diameter of the screw shaft.

Table 2 : Lead and diameter selection

Screw shaft outer diameter	Lead										
	1	2	4	5	6	8	10	12	16	20	24
20				●				●		●	
25				●				●			
28					●						
30											
32								●			
36								●		●	●
40								●			
45									●		
50										●	

●: Standard stock
 ○: Semi-standard stock

So, the maximum speed is obtained from the lead (20mm), it is 1800rpm.

3.2 Pitch and Angle of Thread

1. The Pitch

$$P_h = n_s \times p \tag{3}$$

Where, p is the screw pitch (distance between identical points of two consecutive threads) and n_s is the number of starts.
 So, $p = P_h/n_s = 10\text{mm}$.

2. Angle of Thread

The angle formed by the two sides of the thread (or their projections) with each other.

$$\Psi = 60^\circ$$

3.3 Calculating Length Between Bearing Supports (Shaft Length)

Using Figure (5) and equation (4) for calculation shaft length L :

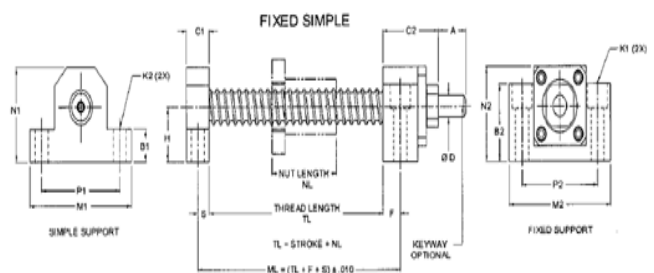


Figure 3: Ball screw method of support

$L = \text{Stroke length} + \text{ball nut length} + s + F + \text{Desired over travel} = 648\text{mm}$ (4)

3.4 Support Method

The supporting method is determined from equation (4) of the screw shaft critical speed.

$$C_s = \frac{F(1.2 \times 10^7) dr}{L^2} \tag{5}$$

Where: C_s is critical speed (rpm). F is end support factor. dr is

root diameter of screw (mm), the value is 31.2mm from table(3). L is length between supports (mm).

So, $F=2$.

The fixed –simple conform to the maximum speed shown the figure (6) is selected.

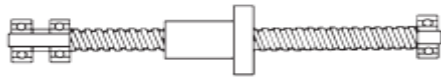


Figure 4: Fixed simple

3.5 Maximum Axial Load

The resultant axial load F_a is given by equation (6 -12):
 Acceleration

$$\alpha = \frac{V_{max}}{t_1} = 6ms^{-2} \quad (6)$$

Below are the axial load calculated when the limb is in:
 Accelerating:

$$F_{a1} = m \cdot g + m \cdot \alpha + f = 8456.667N \quad (7)$$

Constant acceleration increase:

$$F_{a2} = m \cdot g + f = 5256.667N \quad (8)$$

Slow increase:

$$F_{a3} = m \cdot g - m \cdot \alpha + f = 2056.667N \quad (9)$$

Deceleration:

$$F_{a4} = m \cdot g - m \cdot \alpha - f = 1996.667N \quad (10)$$

Constant deceleration decrease:

$$F_{a5} = m \cdot g - f = 5196.667N \quad (11)$$

Slow decrease:

$$F_{a6} = mg + m \cdot \alpha - f = 8396.667N \quad (12)$$

Therefore, the maximum axial load acting on the screw shaft occurs when the limb accelerates up. The value is $F_{max} = Fa1$.

3.6 Rate Of Risk Allowed By The Screw Speed

With reference to table3-3, the coefficients associated with installation of the ball screw shaft is 15.1, as it conform to the supporting method.

Table 3: Coefficients Associated With Installation

S/No.	Fixing Method	λ_1	λ_2
1	Fixed-Free	1.875	3.4
2	Simple-Simple	3.142	9.7
3	Fixed-Simple	3.927	15.1
4	Fixed - Fixed	4.73	21.9

Given Data:

Installation spacing (lb) = (648-130) mm=518mm

Lead screw Axis root diameter , $d_r=31.2$ mm

Calculassions:

$$N = \lambda_2 \times \frac{d_r}{l_b} \times 10^7 = 17557.878 \text{ min}^{-1}$$

4. Nut Selection

The diameter of the screw axis and lead is known, so nut can be selected using C_a (dynamic load rating (N)) and C_{a0} (static load rating (N)).

BLK 3620-5.6 is selected as the nut type. The dynamic load is the load at will achieve the service life of 1×10^6 rev ($C_a=54.9$ KN) and static load rating ($C_{a0}=134.3$ KN) from Table 3.

Table 3: No Preload Type of Precision Ball Screw

Screw shaft outer diameter d	Lead Ph	Model No.	Ball center-to-center dm	Thread minor diameter dc	No. of loaded circuits Rows X turns	Basic load rating	
						C_a kN	C_{a0} kN
36	10	BNF 3610-2.5	37.75	30.5	1×2.5	27.6	63.3
		BNF 3610-5	37.75	30.5	2×2.5	50.1	126.4
		BNF 3610-7.5	37.75	30.5	3×2.5	71.1	190.1
		DK 3610-3	37.75	30.5	3×1	28.8	63.8
		DK 3610-4	37.75	30.5	4×1	36.8	85
	12	BNF 3612-2.5	38	30.1	2×2.5	32.1	71.4
		BNF 3612-5	38	30.1	2×2.5	58.4	142.1
	16	BNF 3616-2.5	38	30.1	1×2.5	32.1	71.4
	20	BNF 3620-1.5	37.75	30.5	1×1.5	17.6	38.3
		BLK 3620-5.6	37.75	31.2	2×2.8	54.9	134.3
	24	BLK 3624-5.6	38	30.7	2×2.8	63.8	151.9
	36	BLK 3636-2.8	37.4	31.7	1×2.8	22.4	54.1
BLK 3636-3.6		37.4	31.7	2×1.8	30.8	78	

So BLK 3620-5.6 is selected as the nut type.

Selecting an end-cap type figure 5, this models achieve stable motion in a high-speed rotation.

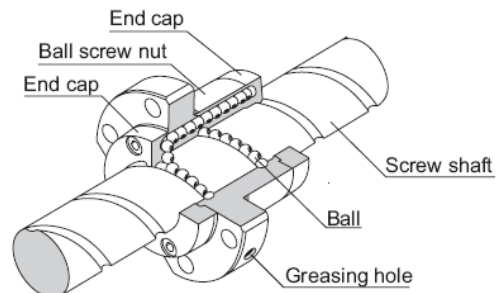


Figure 5: End-cap type

$F_{a_{max}} = \text{Maximum static load (allowable axial load)}$

Table 4: Static safety factors

machineries	Loading conditions	F_s lower limit
General industrial machineries	When there is no vibration or shock	1~1.3
	When there is vibration or shock	2 ~ 3
Machine tools	When there is no vibration or shock	1~1.5
	When there is vibration or shock	2.5~7

$$F_{a_{max}} = \frac{C_{a0}}{f_s} = 67.15KN$$

By comparison, we know that allowable axial load is greater than the maximum axial load 8456.667N, thus this model can meet the requirements.

5. Working Life

It depend on average number of revolutions per minute and rated life which in turns rated life depend on average axial load and maximum axial load and also the average axial load depend on maximum axial load and running distance. Running distance when in acceleration and deceleration

$$l_{1,4} = \frac{V_{max} \times t_1 \times 10^5}{2} = 30mm \quad (15)$$

Running distance with constant velocity increase and constant velocity decrease

$$l_{2,5} = l_s - \frac{V_{max} \times t_1 + V_{max} \times t_3 \times 10^3}{2} = 340\text{mm} \quad (16)$$

Running distance when in slowly acceleration increase and deceleration decrease

$$l_{3,6} = \frac{V_{max} \times t_3 \times 10^3}{2} = 30\text{mm} \quad (17)$$

To sum up, the average axial load is got:

$$F_m = \sqrt[3]{\frac{1}{2 \times l_s} (F_{a1}^3 \times l_1 + F_{a2}^3 \times l_2 + F_{a3}^3 \times l_3 + F_{a4}^3 \times l_4 + F_{a5}^3 \times l_5 + F_{a6}^3 \times l_6)} = 2753\text{N} \quad (18)$$

$$F_m = 5505.51\text{N}$$

5.1 Rated Life

Since dynamic load ratings C_a (see Table 3) and load factor f_w (see Table 5) are known, according to the average axial load F_m , the rated life L can be obtained:

$$L = \left(\frac{C_a}{f_w \cdot F_m} \right)^3 \times 10^6 = 2.35 \times 10^9 \text{ rev} = 2.89 \times 10^9 \text{ rev} \quad (19)$$

Similarly, according to the maximum axial load F_{max} , the rated life L' can be obtained:

$$L' = \left(\frac{C_a}{f_w \cdot F_{max}} \right)^3 \times 10^6 = 6.33 \times 10^8 \text{ rev} = 7.97 \times 10^8 \text{ rev} \quad (20)$$

Table 5: Load Coefficients

Vibration, Impact	Velocity (V)	f_w
Tiny	$V \leq 0.25 \text{ m/s}$	0.5~0.6
Little	$0.25 < V \leq 1 \text{ m/s}$	0.6~0.7
Medium	$1 < V \leq 2 \text{ m/s}$	0.7~1.0
High	$V > 2 \text{ m/s}$	1.0~1.5

5.2 Average Number of Revolutions Per Minute

Since number of times round per minute $n=7\text{min}^{-1}$, and stroke length l_s and lead Ph are known, average number of Revolutions Per Minute can be calculated:

$$N_m = \frac{2 \times n \times l_s}{Ph} = \frac{240 \text{ min}^{-1}}{280 \text{ min}} = 280 \text{ min}^{-1} \quad (21)$$

5.3 Conversion from Revolution to Hours

Since rated life L and the average number of revolutions per minute N_m are known, according to the average axial load, conversion from Revolution to Hours is

$$L_h = \frac{L}{60 \cdot N_m} = \frac{163000h}{60 \cdot 280} = 172023.81\text{hrs} \quad (22)$$

Similarly, according to the maximum axial load, working life is

$$L'_h = \frac{L'}{60 \cdot N_m} = \frac{43960h}{60 \cdot 280} = 47440.476\text{hrs} \quad (23)$$

6. Motor Torque

The frictional torques induced by external loads are:

Constant acceleration:

$$T_1 = \frac{F_{a2} \times ph}{2 \times \pi \times \eta} = 18591.419\text{Nmm} \quad \text{with 90\% efficiency} \quad (24)$$

Constant deceleration:

$$T_2 = \frac{F_{a5} \times ph}{2 \times \pi \times \eta} = 18379.213\text{Nmm} \quad \text{with 90\% efficiency} \quad (25)$$

For acceleration operation

$$T_3 = (J + J_m) \times \omega_b \quad (26)$$

$$J = m \left(\frac{ph}{2\pi} \right)^2 \times i^2 \times 10^{-6} + J_s \times i^2 + J_G + J_I \times i^2 \quad (27)$$

Where: m is Load mass. Ph is Lead. J_1 is Inertia moment of the screw. I is moderating ratio. J_s is Inertia moment of the gear or else on screw. J_G is Inertia moment of the gear or else on motor.

And,

$$J_s (\text{screw}) = D^4 \times \text{length} \times .028 \quad (28)$$

D = diameter of pulley.

$$J_s = 5.7\text{Kgmm}^2$$

Therefore, $J = 5.7162\text{kgmm}^2$.

And,

$$\omega_b = \frac{2\pi \times N_m}{60 \times t} = 293.2\text{rad/s}^2 \quad (29)$$

$$T_3 = (J + J_m) \times \omega_b = 1724.954\text{Nmm}$$

Therefore, the required torques are:

Accelerating:

$$T_{k1} = T_1 + T_3 = 10663\text{N} \cdot \text{mm} = 20316.3\text{Nmm} \quad (30)$$

Constant acceleration increase:

$$T_{t1} = T_1 = 9423\text{N} \cdot \text{mm} = 18591.4\text{Nmm} \quad (31)$$

Slow increase:

$$T_{g1} = T_1 - T_3 = 8183\text{N} \cdot \text{mm} = 16866.5\text{Nmm} \quad (32)$$

Deceleration:

$$T_{k2} = T_2 - T_3 = 7829\text{N} \cdot \text{mm} = 16654.3\text{Nmm} \quad (33)$$

Constant deceleration decrease:

$$T_{t2} = T_2 = 9069\text{N} \cdot \text{mm} = 18379.2\text{Nmm} \quad (34)$$

Slowly decrease:

$$T_{g2} = T_2 + T_3 = 10309\text{N} \cdot \text{mm} = 20104.1\text{Nmm} \quad (35)$$

So, $T_{max} = T_{k1}$.

Table 6: Torque And Time Values

torque	time
T_{k1}	20316.3Nmm
T_{t1}	18591.4Nmm
T_{g1}	16866.5Nmm
T_{k2}	16654.3Nmm
T_{t2}	18379.2Nmm
T_{g2}	20104.1Nmm

$$T_{rms} = \sqrt{\frac{T_{k1}^2 \cdot t_1 + T_{t1}^2 \cdot t_2 + T_{g1}^2 \cdot t_3 + T_{k2}^2 \cdot t_1 + T_{t2}^2 \cdot t_2 + T_{g2}^2 \cdot t_3}{t_1 + t_2 + t_3 + t_1 + t_2 + t_3}} \quad (36)$$

$$= 9275\text{N} \cdot \text{mm} \quad T_{rms} = 18512.41\text{Nmm}$$

Therefore Sizing the Drive Motor is:

- rated torque of the motor must be above T_{rms}
- Maximum operating speed 1800rpm
- Motor rated speed 2000rpm

7. Modeling Using UG6.0

After finishing the calculations, the parts of 3dof parallel manipulator can be modeled by using UG 6.0.

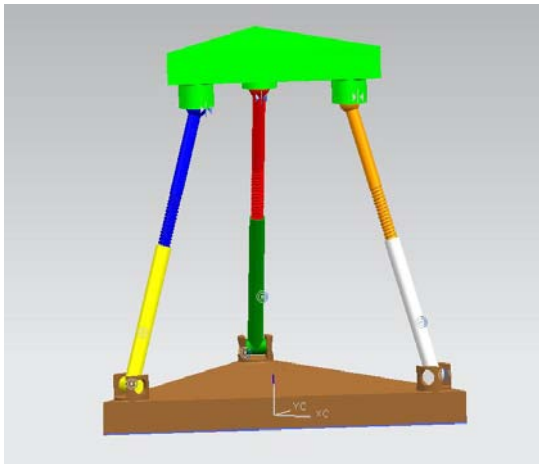


Figure 6: 3 DOF parallel manipulator in UG

8. Simulation In ADAMS

The manipulator is imported to ADAMS and constrains was applied to the model accordingly with the prismatic joint as the actuated joint as in the chart below. Also the friction force was applied to prismatic joint of each limb with gravitational force of 15680N applied to the moving platform centre.also the maximum stroke length is 100mm. For the model in question forces at each prismatic joint was analysed. Two different functions were used i.e. SINE FUNCTION. The result obtained by the two was compared at each stage of simulation.

Note: the model has three motions (Up and down ,Roll ,Pitch). Here we will using roll or pitch in simulation.

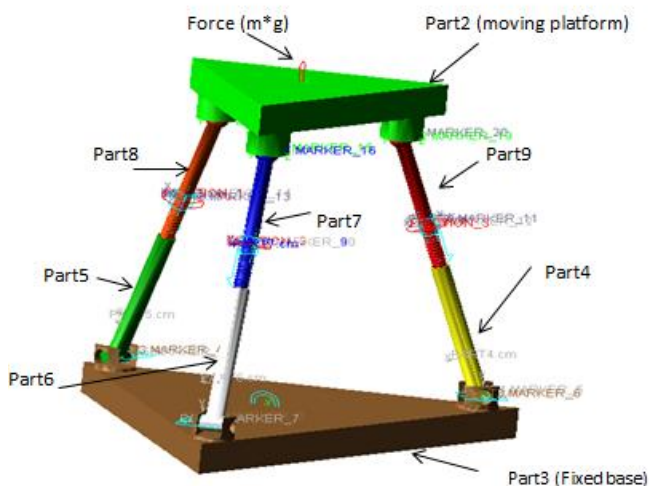


Figure 7: model before the simulation

Table 7: the joints according to fig 5-1 in ADAMS

No of joint	Name of joint	figure	place
1	Fixed Joint		on the part3
2	Revolute joint		Between part3 and part5
3	Revolute joint		Between part3 and part4
4	Revolute joint		Between part3 and part6
5	Translational joint		Between part6 and part7
6	Translational joint		Between part4 and part9
7	Translational joint		Between part5 and part8
8	Spherical joint		Between part2 and part7
9	Spherical joint		Between part2 and part8
10	Spherical joint		Between part2 and part9

8.1 Forces At Prismatic Joints

8.1.1 Sine Function of $1406.536d*(1-\sin(\text{time}))$, $406.536d*(1-\sin(\text{time}))$, and $1406.536d*(1+\sin(\text{time}))$ were used at first, second and third limb to find the position of the moving prismatic joint parts, force at each prismatic joint and orientation of the moving platform.

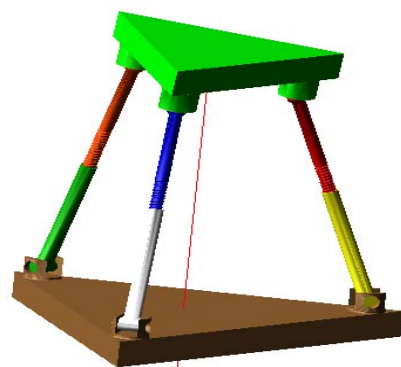
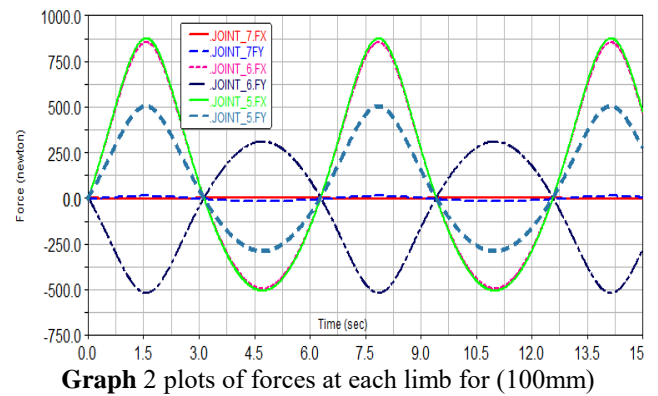
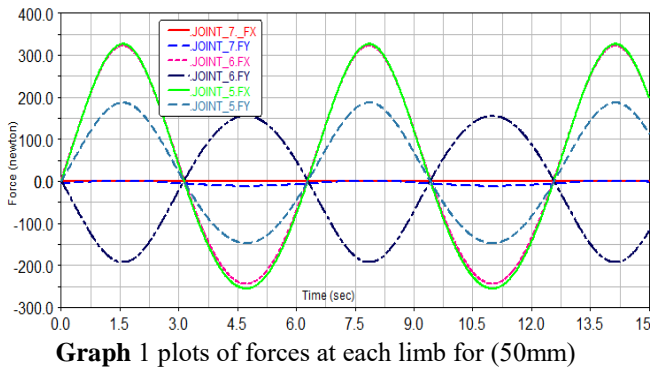


Figure 8: model during the simulation



8.1.2 Sine Function of $2813.071d*(1-\sin(\text{time}))$, $2813.071d*(1+\sin(\text{time}))$, and $2813.071d*(1-\sin(\text{time}))$, were used at first, second and third limb to find the position of the moving prismatic joint parts, force at each prismatic joint and orientation of the moving platform.

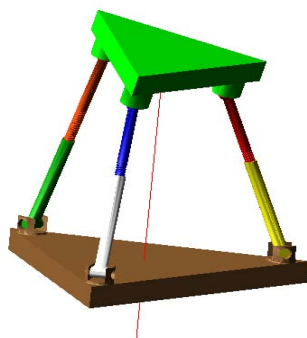


Figure 9: model during the simulation

Table 8: Forces Results

2	1	S/N	
$2813.071d*(1\sin(\text{time}))$	$1406.536d*(1-\sin(\text{time}))$	Functions	
$2813.071d*(1-\sin(\text{time}))$	$1406.536d*(1-\sin(\text{time}))$		
$2813.071d*(1+\sin(\text{time}))$	$1406.536d*(1+\sin(\text{time}))$		
875.52	326.46	Fx Max (N)	Limb 1
-506.75	-255.1759	Fx Min (N)	
502.24	186.947	Fy Max (N)	
-291.8	-147.15	Fy Min (N)	
853.73	322.82	Fx Max (N)	Limb 2
-494.1	-243.876	Fx Min (N)	
-518.77	-192.74	Fy Max (N)	
309.68	155.7	Fy Min (N)	Limb3
-0.64	-0.5	Fx Max (N)	
-0.282	-0.35	Fx Min (N)	
-16.74	-11.089	Fy Max (N)	
12.32	1.435	Fy Min (N)	

9. Conclusion

Design of structure of parallel robotic mechanisms is a key issue in robotic area. In this paper, the structural designs are carried out, such as the screw shaft and nut calculation, the load calculation, the motor specifications selection, according to the given parameters. Then the model is established by using UG 6.0. From forces results in table 8 the forces (Fx, Fy) changed according to the function (stroke length).

10. Appreciation

The work was supported by Scientific Research Development Fund of Tianjin University of Technology and Education (KJY14-02).

References

- [1] L. W Tsai, Robot Analysis: The Mechanics Of Serial And Parallel Manipulators, Wiley, New York, 1999.
- [2] Ginger Shifa, Review and Development of the flight simulator, electro-optical and Control, 1998 (3): 8-12.

- [3] Lung- Wen Tsai , Robot Analysis: The Mechanics Of Serial And Parallel Manipulators, college park Maryland.
- [4] Zafer Bingul and Oguzhan Karahan (2012). Dynamic Modeling and Simulation of Stewart Platform, Serial and Parallel Robot Manipulators - Kinematics, Dynamics, Control and Optimization, Dr. Serdar Kucuk (Ed.), ISBN: 978-953-51-0437-7,
- [5] Ball Screw : General Catalog ,A Technical Descriptions of the Products.
- [6] J.-P. MERLET ,Parallel Robots , Springer,P.O. Box 17, 3300 AA Dordrecht, The Netherlands.